steel research international
www.steel-research.de

Experimental Determination of Slag Emissivities for Enhanced Slag Control by Infrared-Based Systems

Bharath Vasudev Rangavittal, Herbert Köchner, and Björn Glaser*

Dedicated to Prof. Em. Seshadri Seetharaman on the occasion of his 80th birthday

For today's high-quality steel production, good control of slag composition is essential in secondary steelmaking. However, the conventional slag analysis practice, involving sampling, sample preparation, and analysis, is very time-consuming. This work is the first step toward an investigation of infrared (IR)-based systems and can be used for online slag composition monitoring using the principle that different slag compositions have different emissivities in the IR wavelength range. Therefore, this work experimentally determines emissivity values of slags as a function of composition at steelmaking temperature, since available data for slags are very limited in the literature. The emissivities of three different slag compositions belonging to the Al_2O_3–CaO–SiO_2–MgO system are investigated at 1773 K. The investigated emissivities are in the range of 0.75–0.87, with the best repeatability seen in the slag which is fully liquid at 1773 K. Variations in emissivities are observed within the other slags due to the presence of solid phases. Although the data clearly indicate a difference of emissivities as a function of slag composition, further experiments must be performed to evaluate the emissivities of other characteristic slags at different temperatures in order to further assess the applicability of IR-based systems for slag composition control.

1. Introduction

Slag is crucial in secondary steelmaking as it affects the quality of the final product in many ways. A typical secondary metallurgy ladle slag is a four-component system comprising aluminum oxide (Al_2O_3), calcium oxide (CaO), silicon oxide (SiO_2), and magnesium oxide (MgO). Some important functions of slag are steel desulphurization and inclusion control during the secondary refining metallurgical processes. These functions heavily depend on the slag composition, where steel desulfurization is influenced by the slag Al_2O_3/CaO ratio, which has an inverse effect on the sulfur distribution.[1] The MgO content in the slag is also known to affect the dissolution behavior of refractory materials during secondary steelmaking.[2] Moreover, the slag composition also affects slag properties such as viscosity[3] and its liquidus temperature, which can influence the ladle refining operations. Thus, the knowledge and good control of the slag composition during the secondary steelmaking processes is essential for improving product quality and extending refractory lifetime, thereby making the steelmaking process more efficient and sustainable.

The conventional practice of analyzing slag compositions involves sampling, sample preparation, and analysis of sample composition in a remote laboratory. Even with a state-of-the-art sampling system and advanced analytical techniques, some sample preparation is still required, rendering the online analysis and thereby the online control of slag composition difficult with this conventional practice. This leads to potential delays in industrial steel production. Recent studies have investigated the use of laser-induced breakdown spectroscopy (LIBS) in rapid analysis of slag composition.[4–6] These studies have demonstrated the promising potential of LIBS in quick slag analysis within industrial trials. On the other hand, today's infrared (IR)-based camera systems can provide real-time visualization of slag and steel–slag differentiation at steelmaking temperatures. Such systems are already being used in industry to detect and monitor slag carry-over at various stages of steelmaking processes.[7,8] The fundamental principle behind this function of IR-based systems is based on the difference in emissivity in the IR spectrum between liquid slag and liquid steel at steelmaking temperatures. The difference in emissivity increases with increasing wavelengths and reaches its maximum in the spectral range of 8.0–14.0 μm, where atmospheric interference mainly from moisture and carbon dioxide is also low.[8] Although previous literature has verified this principle with experimentally measured emissivity values of liquid slags and liquid steels, there is still a lack of

B. V. Rangavittal, B. Glaser
Department of Materials Science and Engineering
KTH – Royal Institute of Technology
10044 Stockholm, Sweden
E-mail: bvra@kth.se

H. Köchner
ASenSo GmbH
Am Birkengraben 12, 50259 Pulheim, Germany

The ORCID identification number(s) for the author(s) of this article can be found under https://doi.org/10.1002/srin.202400277.

DOI: 10.1002/srin.202400277

data regarding the effect of composition and temperature on emissivity values.[9–11]

It should be emphasized that the emissivity of slag is a thermophysical surface property which is dependent on composition, temperature, and surface conditions besides being affected by other factors such as wavelength.[12] According to the best of authors' knowledge, the effect of composition on the emissivity of liquid slag has not yet been investigated. The authors believe that future knowledge on emissivity values in the IR range for different slag compositions at steelmaking temperatures could be very useful for online assessment of slag compositions by IR-based camera systems. Nevertheless, such data are also essential for the development of accurate process models involving slags for various applications.

This study explores the first step toward investigating the applicability of IR-based systems for online slag composition assessment during secondary steelmaking. This work presents the experimental determination of emissivity values in the IR range for slags of different compositions at steelmaking temperature using a laboratory-scale furnace. Three different slag compositions belonging to the high-CaO-containing region of the quaternary system Al_2O_3–CaO–SiO_2–MgO have been chosen to resemble a typical ladle slag for the investigation.

2. Experimental Section

The experimental setup used for high-temperature emissivity investigations of slags is shown in **Figure 1**. A vertical tube furnace with resistance heating elements having a maximum operating temperature of 2073 K was used. The furnace was controlled by a Eurotherm controller by means of a type B thermocouple (Pt—6% Rh/Pt—30% Rh) located near the furnace heating elements. The reaction tube, made of high-purity (99.8%) alumina, was sealed at both ends using Viton or Silicone *O*-rings to prevent oxygen from entering the furnace tube. The reaction tube was cooled on both ends by water-cooled aluminum chambers. The hot zone of the furnace, defined as a uniform temperature zone with a variation of ±2 K, was estimated to be 3 cm in height. A molybdenum (Mo) crucible with an inner diameter of 71 mm was used together with a crucible holder of the same material. A type C thermocouple (W—5% Re/W—26% Re) was mounted inside the crucible holder with its tip located just below the crucible to monitor the temperature of the sample. Both crucible with the slag (slag height 6 mm) and the tip of type C thermocouple were positioned inside the furnace hot zone to ensure accurate temperature control. A zinc selenide (ZnSe) optical window of thickness 6 mm, with optical transmission in the required wavelength range of 0.6–21.0 μm, was mounted on the top of the furnace to observe the sample surface within the IR wavelengths. The optical window was placed at the shortest possible height of 430 mm from the hot zone of the furnace to minimize unwanted reflection of thermal radiation of the inner walls of the reaction tube from the sample surface that could possibly lead to the appearance of a black body on the entire sample surface. This approach was verified by conducting a trial with a molten carbon steel sample at steelmaking temperature, on which the effect of the reflection of the thermal radiation of the tube inner walls can be more pronounced due to its much lower emissivity than slag. The trial revealed an emissivity value of 0.27, which closely agreed with the widely accepted value of 0.28 for mild steel in the temperature range of 1873–2073 K.[13,14] This confirmed that the effect of the radiations from the furnace tube inner walls was minimized, when the sample surface was observed from the chosen height of 430 mm.

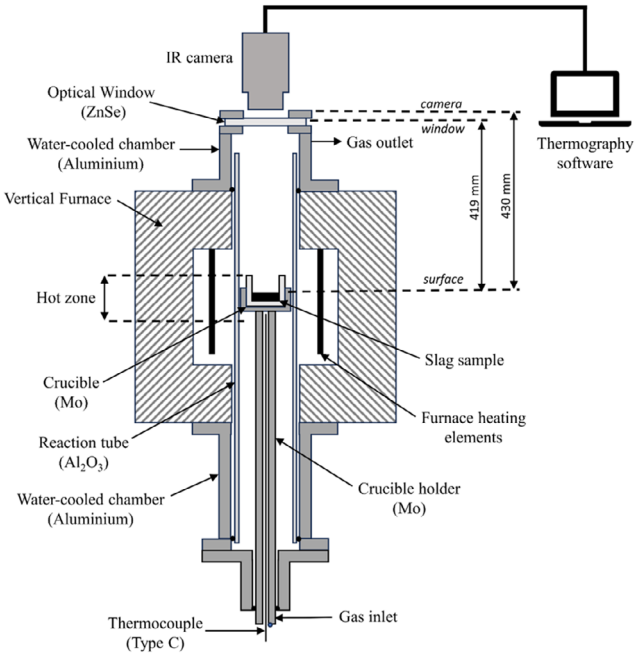

Figure 1. High-temperature experimental setup for emissivity investigations.

High-purity argon (Ar) gas (>99.999%) was used to establish and maintain an inert environment inside the furnace tube during the experiments. The flow of Ar gas to the furnace was controlled using a Bronkhorst mass flow controller. The sample temperature measured by type C thermocouple during the experiment was read using an INOR temperature transmitter. The transmitter was connected to a computer, where the temperature was continuously logged in a file using INOR's proprietary software, Ipro 4.31.10. A calibrated Infratec VarioCAM HD infrared camera (IR camera) with a resolution of 640 × 480 IR pixels and a spectral detection range of 7.5–14.0 μm was used for capturing IR images of the sample surface. The camera was calibrated for high-temperature measurements up to 2073 K. The IR camera was fit with a lens of 20 mm focal length that can provide a focusing range of more than 300 mm. The IR camera was connected to a computer using a GigE interface and controlled by Infratec's proprietary thermographic software package, IRBIS3.1 professional.

2.1. Sample Preparation

Commercially available aluminum oxide (Al_2O_3), calcium oxide (CaO), silicon oxide (SiO_2), and magnesium oxide (MgO) powders of at least 99% purity were considered for the preparation of the slag samples. The different oxide powders were carefully mixed using mortar and pestle for at least 1 h to prepare a homogenous synthetic slag mixture. The powder mixture was

then hydraulically pressed into slag pellets. These pellets were premelted in a graphite crucible using an induction furnace. The liquid slag was then poured into a molybdenum crucible for solidification. All slag samples for the high-temperature emissivity investigations were subjected to premelting to achieve a homogenous composition. For this work, samples of three slag compositions belonging to the Al_2O_3–CaO–SiO_2–MgO quaternary system were prepared in this manner and were sent for composition analysis by X-ray fluorescence (XRF) technique.

2.2. Experimental Procedure

The mass of the premelted samples for the experiments was measured to be between 55 and 60 g. Prior to heating, the reaction tube was evacuated with a vacuum pump for 1 h and then filled with argon gas twice to completely remove oxygen from the furnace tube in order to avoid oxidation of both the crucible and the crucible holder. After refilling, the argon gas flow rate to the furnace was fixed at 0.1 L min^{-1} by the Bronkhorst mass flow controller for all experiments. The heating program was started on the Eurotherm controller at a maximum heating rate of 2 K min^{-1}. The sample was heated at least 5 K above the target temperature of 1773 K before being reduced to 1773 ± 0.5 K to ensure an equal temperature distribution within the sample. When the target temperature was stabilized within ± 0.5 K, the IR camera was positioned very close to the window within a distance of 5 mm to capture the thermographic images of the slag surface using IRBIS3.1 professional software. After successful completion of the experiment, the sample was sent for composition analysis by XRF technique.

2.3. Emissivity Calculations

The IR camera measures infrared radiation emitted by a target surface, which is defined as spectral exitance, $M(T)$, given by

$$M(T) = \varepsilon M_{BB} \tag{1}$$

where ε is the emissivity of the target surface and $M_{BB}(T)$ is the spectral exitance of a theoretical black body calculated by Planck's law.

$$M_{BB}(T) = \int_{\lambda_1}^{\lambda_2} C_1 \lambda^{-5} \left(e^{\frac{C_2}{\lambda T}} - 1 \right)^{-1} d\lambda \tag{2}$$

where λ_1 and λ_2 are spectral wavelength limits of the IR camera, C_1 and C_1 are radiation constants, and T is the temperature of the target. In the presence of an optical window in the radiation path, the transmissivity τ_w should also be considered in the expression for spectral exitance. If the optical window has extremely low IR absorption and when IR camera is placed very close to the window, Equation (1) becomes

$$M(T) = \tau_w \varepsilon M_{BB} + (1 - \tau_w) M_C \tag{3}$$

where M_C is the black body spectral exitance corresponding to the camera temperature. T_C is again given by Planck's law.

$$M_C(T_C) = \int_{\lambda_1}^{\lambda_2} C_1 \lambda^{-5} \left(e^{\frac{C_2}{\lambda T_C}} - 1 \right)^{-1} d\lambda \tag{4}$$

where T_C can be obtained from the IRBIS3 professional software. The emissivity of the target surface can then be calculated by rearranging Equation (3) to give

$$\varepsilon = \frac{M - M_c}{\tau_w M_{BB}} - \frac{M_c}{M_{BB}} \tag{5}$$

In this work, the thermographic images captured by IR camera contained spectral exitance measured at each image pixel. A region was selected on the image of the slag surface, from which the spectral exitance data was extracted for each pixel. The extracted data were then used to calculate emissivity using Equation (5) with the help of a Python code. The parameters used for the emissivity calculations are listed in **Table 1**.

3. Results and Discussion

Table 2 shows the experimental matrix used in the study, along with the sample composition analyzed before (as premelted) and after the high-temperature experiment by XRF. As mentioned earlier, the three slag samples (Slag A, Slag B, and Slag C) studied in this work belong to the Al_2O_3–CaO–SiO_2–MgO quaternary system. Sample A4 failed during experiment and was therefore not further sent for analysis. Due to the premelting procedure in a graphite crucible, the carbon content in the

Table 1. Parameters for emissivity calculation.

Parameters	Value	Unit
C_1	3.742×10^8	W μm^4 m^{-2}
C_2	1.439×10^4	μm K
λ_1	7.5	μm
λ_2	14.0	μm
τ_w	0.71	–
T	1773	K
T_C	303–313	K

Table 2. Analyzed slag sample composition.

Slag ID	Sample ID	Before experiment [Mass%]				After experiment [Mass%]				Max T [K]
		Al_2O_3	CaO	SiO_2	MgO	Al_2O_3	CaO	SiO_2	MgO	
A[a)]	A1	35.6	38.6	17.9	7.9	34.5	40.1	17.5	7.9	1788
	A2	35.6	38.2	18.4	7.8	34.7	39.3	17.9	8.1	1775
	A3	36.0	37.8	18.2	7.9	33.8	39.3	18.8	8.1	1784
B	B1	35.4	43.9	14.1	6.6	34.4	43.6	15.6	6.4	1787
	B2	35.3	43.9	14.2	6.6	35.1	43.9	14.4	6.6	1783
	B3	35.4	43.6	14.5	6.5	35.7	42.9	14.9	6.5	1784
	B4	35.4	44.1	13.9	6.6	34.8	43.9	15.0	6.2	1781
C	C1	44.3	42.6	8.7	4.5	43.9	42.2	9.3	4.6	1799
	C2	44.0	43.0	8.6	4.4	43.6	42.3	9.4	4.7	1797
	C3	44.8	42.2	8.6	4.3	44.9	41.7	8.8	4.6	1780
	C4	45.2	41.3	8.8	4.7	44.8	41.9	8.6	4.7	1779

[a)]Sample A4 not analyzed because of experimental failure.

premelted samples before the experiment was analyzed to be less than 0.1 mass% for each sample; therefore, its effect on this investigation was considered to be negligible. Similarly, the presence of molybdenum (Mo) pickup in the form of oxides or free metal in the samples after the experiment was analyzed to be less than 0.15 mass%. Due to the very low amount of Mo in the samples, its effect on the experimental result was also considered to be negligible. The composition of all the slag samples was consistently repeated. Moreover, the change in the concentration of each oxide experienced by the slag samples after the experiment was found to be within the analysis errors, which are ±2 mass% for the analysis of Al_2O_3 and CaO, ±1 mass% for the analysis of SiO_2, and ±0.5 mass% for the analysis of MgO. Furthermore, Table 2 also reports the slightly varying maximum temperature reached per sample. It can also be seen that the difference between the highest and the lowest maximum temperature recorded is observed to lie within the measurement error, which is ±1% of the measured value for the type C thermocouple used for sample temperature control during the experiment. The slight temperature fluctuations were caused due to furnace reaching its upper operation limit during the experiments.

Figure 2 shows examples of the thermographic (IR) images of the high-temperature furnace captured by the IR camera at 1773 ± 0.5 K. Each image exhibits measurements of spectral exitance (M) at each pixel in the spectral range of 7.5–14.0 μm and is colored according to the scale shown on the right side of the image, which indicates the exitance values. It should be noted that the image also depicts other furnace components (such as the reaction tube and the crucible) surrounding the slag sample (denoted as R1).

To identify the slag, the number of pixels, N corresponding to the slag surface in the IR image was calculated by

$$N = \frac{A_s}{\mathrm{IFOV}^2} \tag{6}$$

where the slag surface area A_s was calculated from the inner radius (r) of the crucible. The instantaneous field of view (IFOV), which describes the spatial resolution, is defined as the size of the target represented by 1 pixel of the IR camera system including lens. The value of IFOV was 0.3814 mm, obtained from Infratec according to the distance of the slag surface from the IR camera, which is 430 mm for all the samples. Thus, the number of pixels corresponding to the slag surface was calculated to be 27 200 pixels, resulting in an equivalent number of spectral exitance measurements for each sample at 1773 ± 0.5 K. **Table 3** presents the mean and standard deviation (SD) of measured spectral exitance from the slag surfaces (represented as R1 in Figure 2) for all samples. It is evident that the variations in the measurements, as indicated by the SD, are reduced when considering a smaller region (shown as R2 in Figure 2) at the center of the slag surface for all samples. This smaller region only contained 2145 pixels, corresponding to a surface area of 319 mm^2 (a circle of 10 mm) on the slag surface. The larger variations in the measurements observed in R1 are caused by the unavoidable effects of reflections from the inner walls of the tube and the crucible walls on the measurement of spectral exitance from the slag surface. Due to lower variations in spectral exitance measurements, R2 was considered as the region of interest (ROI) for the emissivity calculations for all slag samples.

Emissivity values were computed at each pixel in R2 for each sample from their spectral exitance measurements using Equation (5) and the values are given in Table 1. A mean emissivity value was then calculated for each sample. **Figure 3** presents a plot of the average emissivity values calculated for all samples at 1773 ± 0.5 K in the spectral range 7.5–14.0 μm

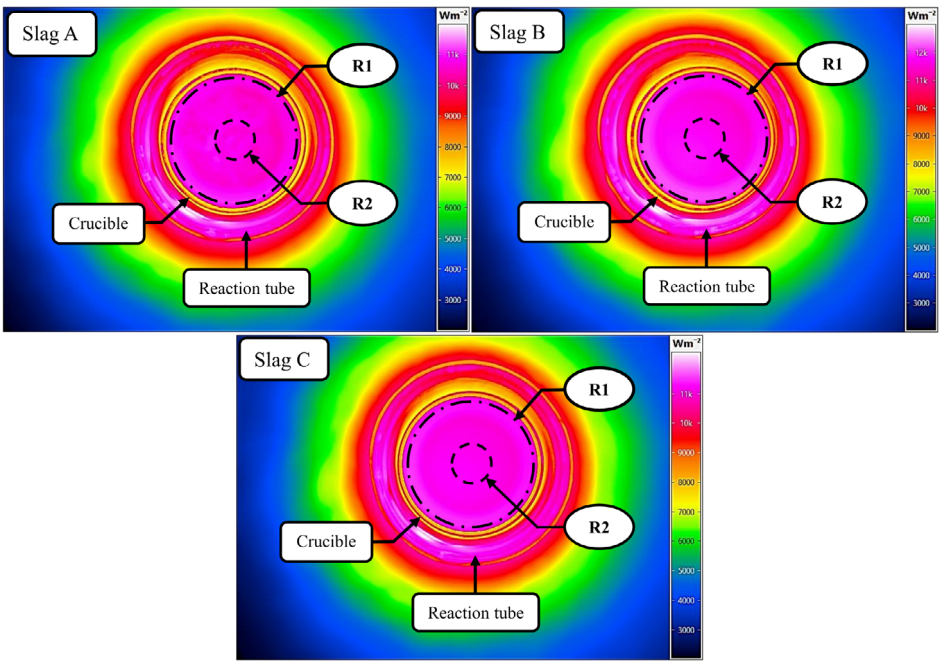

Figure 2. Thermographic (IR) images of the high-temperature furnace containing slag samples; R1: Slag surface (27 200 pixels), R2: ROI (2145 pixels) for emissivity calculation.

Table 3. Spectral exitance measurements for slag samples by IR camera in the R1 and R2 regions.

Sample id	Spectral exitance [M] [Wm^{-2}] (at 1773 ± 0.5 K)			
	Mean		Standard deviation	
	R1	R2	R1	R2
A1	10 719	10 733	157	84
A2	11 902	11 789	154	33
A3	10 507	10 487	115	55
B1	11 043	11 070	171	55
B2	11 766	11 747	195	66
B3	10 254	10 251	117	31
B4	11 022	11 075	142	35
C1	11 382	11 333	154	42
C2	11 190	11 183	143	41
C3	11 306	11 344	132	34
C4	11 409	11 393	138	36

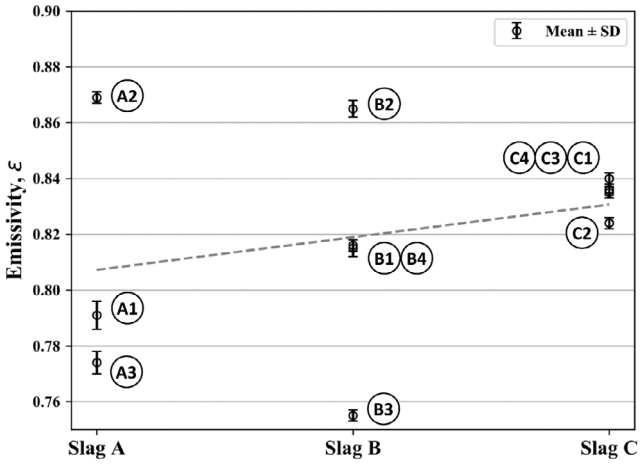

Figure 3. Calculated mean emissivity values with SD of slag samples at 1773 ± 0.5 K in spectral range of 7.5–14.0 μm in region R2, 319 mm^2 (Each data point is labeled with its corresponding sample number).

considering the region R2. The emissivity values observed lie in the range of 0.75–0.87. It is worth mentioning that in Equation (5), $M \approx \text{MBB} \approx O(10^4)$ and $M_C \approx O(10^2)$ for all the samples. This arises because the camera temperature is very low when compared to the target temperature, whereby the effect of reflection from the IR camera, given by M_C in the emissivity calculation, is negligible. The error caused by the calculated emissivity values in this work upon removing M_C from Equation (5) would be in the order of magnitude of 10^{-3}. **Table 4** shows the emissivity values of slags at steelmaking temperatures reported in the literature. Due to the lack of information regarding temperature and composition in literature (Table 4), it was difficult to make a direct comparison of findings in this work with the findings in literature. It was also observed that the emissivity values reported in literature differ a lot from each other, which is maybe caused by the different measurement

Table 4. Literature emissivity values for slags in the temperature range 1673–1923 K.

Emissivity value	Spectral range [μm]	Temperature [K]	Process	References
0.90	7.5–14.0	1923	BOF	[9]
≈0.80	7.5–14.0	–	VD	[10]
0.64–0.68	7.5–14.0	1673–1873	–	[11]

and experimental conditions used. However, it is worth mentioning that the emissivity values in Table 4 did not greatly differ from the literature values and best agreed with those reported by M. Nadif et al.,[10] with about 80% of the values falling within an interval of ±0.05 from emissivity 0.8.

As opposed to a single-emissivity value reported in literature for slag at a fixed temperature and wavelength, a range of emissivity values were produced in this work, indicating the dependence of slag composition on emissivity. Although an apparent increasing trend in emissivity values was observed from Slag A to Slag C, repeatability in the data was best observed among Slag C samples, where three of the four samples exhibited an emissivity value of 0.84 and only sample C2 slightly lower by 0.02. On the other hand, larger variations were observed in emissivity values among the Slag B samples, whereas for Slag A, sample A2 exhibited considerably higher emissivity than the other two. It must be emphasized that the emissivity value calculated from the experiments is a surface property of the different slag samples. Thus, the spread in the calculated emissivity values among Slag A and B samples could be caused by differences in surface conditions within the different samples concerning composition and temperature. Factsage 8.2 was used to determine the equilibrium phases present in the slag samples to better understand their surface condition at 1773 K.

The databases used for equilibrium phase calculations were FactPS, FToxide, and FTmisc, and the premelted sample composition analyzed before the experiment (Table 2) was considered for these calculations. The calculations showed that among the slag compositions, only Slag C samples are completely liquid at the target temperature, whereas Slag A and Slag B samples exhibit the presence of some solid phases at the same temperature. In Slag A, melilite (≤26% by mass) and spinel (7–16% by mass) phases are shown to precipitate, whereas Slag B contains a spinel phase of at most 5% by mass. It should be noted that the errors introduced by the temperature measurements and the composition analysis were considered in the Factsage calculations, which is reflected in the range obtained for the solid phases. Moreover, the liquidus temperatures for Slag A samples are found to be at least 1873 K, which is higher than the maximum temperature that could be reached in the experiments. Therefore, Slag A samples never melted completely during the experiment, irrespective of whether they attained their equilibrium phases. The same cannot be said with certainty for the Slag B samples, as some compositions within the analysis error are revealed to be completely molten at temperatures lower than the target temperature.

Since all of the Slag C samples were completely liquid at 1773 K, the bulk composition and temperature of the slag samples are expected to be homogenous within the sample surface

having the same composition and temperature as the bulk. This also renders a steady surface with little-to-no variations in composition and temperature on the surface among the different Slag C samples. This uniform nature of the surface among all the Slag C samples is reflected in the repeatability of the investigated emissivity values for the Slag C samples except C2, which could be attributed to experimental error. However, for Slag A and Slag B samples, the likely presence of solid phases at the target temperature could introduce inhomogeneity in the bulk composition of the sample with the liquid and the solid phases having different compositions. This inhomogeneity in composition is more noticeable in the case of slag A samples because of the precipitation of larger amounts of solid phases (spinel and melilite) as shown with the Factsage equilibrium calculations. **Table 5** presents the equilibrium composition of liquid phase for Slag A samples at 1773 K. While the presence of solid phases could also cause inhomogeneity in the bulk temperature due to differences in the thermal conductivities of solid and liquid phases, this is not valid in this case as both the thermocouple tip (measuring the sample temperature) and the entire sample were positioned in the uniform-temperature hot zone of the furnace.

The composition at the surface of the sample shall be that of the liquid phase as it is expected to float on top because of the density difference. While the liquid phase floats, the surface may still not attain the equilibrium composition of the liquid phase because of very slow mass transfer due to diffusion and the absence of convection. While the values of diffusion coefficients (D) specific to the investigated slags in this work are not known, studies reveal that they are commonly of the order of magnitude, 10^{-9}–10^{-11} m^2s^{-1}, depending on the slag composition and the diffusion of oxide particles.[15–18] Therefore, in the presence of solid phases in the slag, the surface composition may need a few hours to reach the equilibrium composition of the liquid phase. However, the samples were held at the target temperature for 2–3 min before the IR measurement was done. Therefore, surface equilibrium composition could not be achieved before IR measurement because performing the measurement after such long durations was not feasible due to unavoidable gradual deposition of a very small amount of MoO_3 residue on the optical window surface inside the furnace, interfering with the spectral exitance measurements. Therefore, surface composition resulting from the presence of solid phases taking the analysis and the measurement error into account could be different among the Slag A and Slag B samples, explaining the variation in emissivity values exhibited by them. Despite selecting a smaller region R2 for emissivity calculations, it becomes apparent that the area selection does not change the significance of the effect of solid phase presence on the emissivity calculation. For example, this is illustrated for Slag A samples in **Figure 4** because Slag A contains the highest amount of solid phases at the experimental temperature according to the Factsage equilibrium calculations. The calculated mean emissivity values for Slag A samples in the regions R1 and R2 closely align with each other with a slightly higher error noticed for emissivity calculated in R2. More importantly, the emissivity data variations among Slag A samples were observed to be the same between regions R1 and R2. The resulting negligible effect of area selection on solid phase precipitation and its effect on emissivity calculation was also confirmed with the Slag B samples.

Table 5. Equilibrium composition of liquid phase for slag a given by Factsage at 1773 K.

Sample ID	Equilibrium composition of liquid phase [mass%]			
	Al_2O_3	CaO	SiO_2	MgO
A1	30.9	43.9	19.2	6.0
A2	30.5	43.7	20.0	5.8
A3	29.6	43.6	20.9	5.9

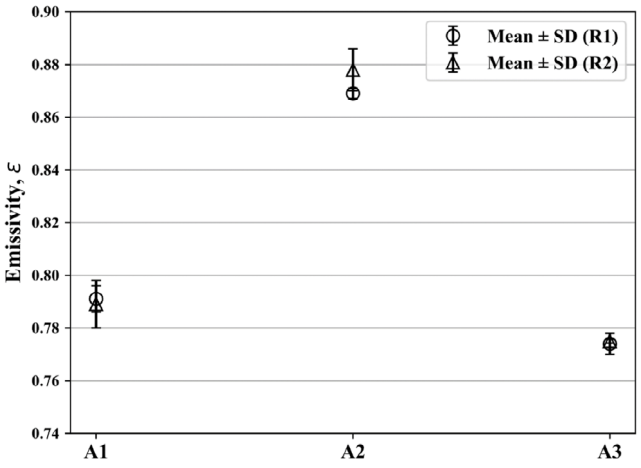

Figure 4. Calculated mean emissivity with SD of Slag A samples in regions R1 and R2.

While the above discussion qualitatively brings out the possible strong influence of the precipitation of solid phases in determining the surface condition of liquid slag, its effect on emissivity values is still not clearly understood. This will, in turn, affect the accuracy of the determination of emissivity values for slag samples containing solid phases. For further experimental investigations in the laboratory, it is recommended to have homogenous and stable surface conditions for accurate emissivity investigations of slags at steelmaking temperatures. This can only be achieved when the slag is in a full liquid state. While the objective was to have the slag in a fully liquid state initially, precipitation of solid phases in some samples was inevitable in this work due to the experimental limitations. In fact, for industrial applications in future, further investigations of the effect of solid phases on the emissivity values would be important, since in industry due to temperature differences, solid phases are always present within the slag layer. In addition, unlike in our work, the environmental conditions are not controlled well in an industry. Therefore, future research on the influence of environmental factors such as the presence of moisture and other volatile matter on the determination of emissivity values will be equally important for industrial applications. While this work showed a discernible effect of composition on the emissivity values of slag, further experiments on other slag compositions and at different temperatures are required to evaluate the applicability of emissivity data for online qualitative assessment of slag composition by IR-based systems in secondary steelmaking. Compared to the recent works[4–6] on LIBS, which successfully demonstrated its

application on solid slag samples as a localized method, our work lays the foundation for potential online analysis of liquid slag over relatively large surface areas using the imaging capability of IR-based systems.

4. Conclusion

This work, as per the authors' best knowledge, presents a first attempt at the experimental determination of emissivity values of three different slag compositions belonging to the quaternary slag system of Al_2O_3–CaO–SiO_2–MgO at steelmaking temperatures in a laboratory-scale furnace. The calculated emissivity values observed for all slag samples are within 0.75–0.87 at 1773 ± 0.5 K in the spectral range of 7.5–14.0 μm. While the experimental data indicated a dependence of emissivity on the slag composition, good repeatability was observed within the Slag C samples which exhibited an emissivity value of 0.84, whereas variations in calculated emissivity values were observed in the other two slag compositions. Since emissivity is a surface property, the surface equilibrium conditions of the slag samples have been investigated using Factsage 8.2. The equilibrium phase calculations showed the presence of solid phases in the samples at 1773 K for the slag compositions which exhibited variations in emissivity values, whereas the sample which showed good repeatability was shown to be fully liquid at 1773 K. The repeatability in emissivity values could therefore be related to a stable and homogenous surface composition, which was possible due to the fully liquid state of one slag sample during the measurement within the measurement time frame. From this work, it can be understood that the precipitation of solid phases could have caused variations in the surface compositions among the other two slags which do not attain equilibrium composition, which is reflected in the spread of their emissivity values. Therefore, it is recommended for further laboratory investigations that slag samples used should be totally liquid without solid remains to accurately determine accurate emissivity values at experimental temperature. The effect of solid phase presence on the surface emissivity is not clearly understood and would be more important to investigate as this is closer to the real industrial situation. While this work showed a noticeable effect of composition on the emissivity of liquid slag, further work on other characteristic slag compositions and at different temperatures is required to assess the applicability of IR-based systems for enhanced slag control during secondary steelmaking processes. This work also emphasizes the effect of slag surface conditions with solid phases on emissivity, which must be investigated in detail in future.

Acknowledgements

This work was financially supported by Vinnova, Sweden's innovation agency, and German Federal Ministry for Economic Affairs and Climate Action (BMWK) through its Central Innovation Programme for SMEs (ZIM). The authors would like to express their gratitude to Degerfors Laboratorium AB for supporting this work with composition analysis of the slag samples.

Conflict of Interest

The authors declare no conflict of interest.

Data Availability Statement

The data that support the findings of this study are available from the corresponding author upon reasonable request.

Keywords

emissivities, high temperatures liquid slags, process controls, slag controls, steelmaking

Received: April 3, 2024
Revised: September 3, 2024
Published online:

[1] M. A. T. Andersson, P. G. Jönsson, M. Hallberg, *Ironmaking Steelmaking* **2013**, *27*, 286.
[2] S. Jansson, *Doctoral Thesis*, KTH Royal Institute of Technology, Stockholm, Sweden **2008**.
[3] P. G. Jönsson, L. Jonsson, D. Sichen, *ISIJ Int.* **1997**, *37*, 484.
[4] J. Petersson, M. Gilbert-Gatty, A. Bengtson, *J. Anal. At. Spectrom.* **2020**, *35*, 1848.
[5] J. Peterson, M. Gilbert-Gatty, K. Ekstrom, L. Hagesjo, A. Bengtson, *Appl. Spectrosc* **2023**, *77*, 907.
[6] S. J. Long, M. G. Li, J. J. Zhou, T. L. Zhang, H.-S. Tang, H. Li, *Chinese J. Anal. Chem.* **2023**, *51*, 100210.
[7] P. Patra, A. Sarkar, A. Tiwari, *Ironmaking Steelmaking* **2019**, *46*, 692.
[8] B. Chakraborty, in *BOF Slag Detection Using Long Wave IR Camera, Paper presented at the Inframation*, Las Vegas, NV, October **2009**.
[9] G. R. Peacock, *Proc. SPIE* **2000**, *4020*, 50.
[10] European Commission, in *Online Control of Desulphurisation and Degassing Through Ladle Bubbling Under Vacuum (ONDECO)—Final Report*, Directorate-General for Research and Innovation, Publications Office, Brussels **2012**.
[11] B. V. Rangavittal, H. Köchner, E. Stark, B. Glaser, *Steel Res. Int.* **2024**, *95*, 2300271.
[12] D. P. DeWitt, G. D. Nutter, *Theory and Practice of Radiation Thermometry*, Wiley, New York, NY **1988**, pp. 40–43.
[13] *Emissivity of Common Materials*, https://www.omega.co.uk/literature/transactions/volume1/emissivitya.html (accessed: February 2024).
[14] *Emissivity Table*, https://kleiberinfrared.com/index.php/en/applications/emissivity.html (accessed: February 2024).
[15] Y. Min, D. Y. Wang, M. F. Jiang, *Adv. Mater. Res.* **2011**, *284–286*, 411.
[16] S. Michelic, J. Goriupp, S. Feichtinger, Y. B. Kang, C. Bernhard, J. Schenk, *Steel Res. Int.* **2016**, *87*, 57.
[17] B. J. Monagahan, S. A. Nightingale, L. Chen, G. A. BRooks, in *7th Int. Conf. on Molten Slags, Fluxes and Salts,* The South African Institute of Mining and Metallurgy, South Africa **2004**.
[18] S. Maroufi, S. Amini, S. Jahanshahi, O. Ostrovski, in *Proc. of The 10th Int. Conf. on Molten Slags, Fluxes and Salts (MOLTEN16)*, The Minerals, Metals & Materials Society-TMS, Pittsburgh, USA **2016**.